

Characterization of ZnSe Thin Film Electrodeposited at Room Temperature in Aqueous Medium without Complexing Agents

Sevda Ildan Ozmen^{1,a,*}¹Advanced Technology Education Research and Application Center, Mersin University, Mersin, Türkiye

*Corresponding author

Research Article

History

Received: 20/03/2024

Accepted: 23/09/2024



This article is licensed under a Creative Commons Attribution-NonCommercial 4.0 International License (CC BY-NC 4.0)

ABSTRACT

This study includes a simple electrodeposition technique for the fabrication of ZnSe thin film at room temperature and in an aqueous medium without additional complexing agents. Comprehensive analysis of the optical, structural, and morphological characteristics of the ZnSe thin film electrodeposited onto an ITO substrate was conducted using UV-Vis spectrometry, X-ray diffraction (XRD), Raman spectroscopy, Fourier transform infrared spectroscopy (FT-IR), and field emission-scanning electron microscopy (FE-SEM). Furthermore, the photoelectrochemical properties were evaluated through current-time (I-t) measurements and electrochemical impedance spectroscopy (EIS) under light on/off conditions. Mott-Schottky analysis was also performed to determine the conductivity type, carrier concentration, and flat band potential of the ZnSe thin film. Structural investigations revealed that the ZnSe thin film has a hexagonal structure, the longitudinal optical (LO) phonon mode, stretching and bending vibration modes of Zn-Se. The carrier type of the ZnSe thin film was identified as n-type semiconductor and photoelectrochemical measurements exhibited a photoresponse under the light illumination.

Keywords: Electrodeposition, ZnSe, Characterization, Mott-Schottky, Photoelectrochemical measurements.sevdaildan@mersin.edu.tr<https://orcid.org/0000-0002-4222-0330>

Introduction

Metal chalcogenides represent a crucial class of semiconductor materials, drawing substantial interest owing to their diverse applications in optics and electronics. Modern electronic devices, such as transistors, diodes, integrated circuits, photovoltaic cells, and other solid-state components, rely on thin-film materials. These materials are often made from metal chalcogenides. Zinc Selenide (ZnSe) that belongs to the II-VI metal chalcogenide family is a significant material in many technological applications because of its broad optical transmission range from the visible to the far infrared region (0.5–22 μm), high transparency, semiconductor properties, and mechanical durability. ZnSe is used for CO₂ lasers, and infrared (IR) optical systems such as lenses, mirrors, and windows [1,2]. Due to its direct and wide energy band gap of 2.7 eV and its semiconductor properties, ZnSe thin films are also important materials for use in optoelectronic devices, light-emitting technologies, and as a buffer or window layer in thin film solar cells [2–5].

Many deposition techniques have been explored to fabricate ZnSe thin films such as chemical bath deposition (CBD) [6,7], closed space sublimation [8,9], pulsed laser ablation deposition (PLAD) [10], and electrochemical deposition (ECD) [11–14]. Among these, ECD has emerged as a particularly noteworthy technique for growing semiconductor films, offering advantages such as cost-

effectiveness, controllability of film properties (such as thickness, morphology, and structure), and the ability to produce large-area devices at low temperatures [3,4,15]. In the ECD method, the properties of the films can be controlled by adjusting various parameters such as applied potential, electrolyte composition and concentration, pH, temperature and deposition time [2,3,15]. The ZnSe thin films were synthesized by ECD method conducted within a temperature range of 50 to 75 °C successfully in earlier studies [3–5,13,15,16].

The ZnSe thin films were deposited on ITO substrates at room temperature by ECD and without additional complexing agents in this study. The comprehensive characterization of ZnSe thin films were carried out with optical, structural, morphological, and photoelectrochemical analysis. Additionally, the determination of the carrier type in the ZnSe semiconductor thin film was achieved through Mott-Schottky analysis.

Materials and Methods

The electrochemical deposition of the ZnSe film onto an ITO substrate was achieved in aqueous solution including 0.1 M ZnCl₂ and 0.1 mM SeO₂ employing the chronopotentiometry technique cathodically. The pH of the solution adjusted to \sim 2 using 1 M HCl and the ECD was carried out at a constant cathodic current of 0.1 mA with

two 30-minute electrodeposition cycles (near -0.65 V) at room temperature. Before coating the ITO substrate and after each deposition cycle, the electrodeposited ZnSe films on the ITO substrates were rinsed with ethanol and ultrapure water, and then dried with an air drier.

To determine the energy band gap value of the ZnSe film, a Shimadzu UV-1100 spectrometer was used. The structural analysis of the ZnSe film was performed using a Rigaku Smart Lab X-ray diffractometer (XRD) with CuK α radiation ($\lambda = 1.54 \text{ \AA}$), an In Via Qontor Raman spectrometer, and a Perkin Elmer UATR Two Fourier transform-infrared (FT-IR) spectrophotometer. Morphological analysis was conducted using a FEI Quanta 650 field emission scanning electron microscopy (SEM) instrument.

The electrochemical (EC) measurements such as current-time (I-t) curves and electrochemical impedance spectroscopy (EIS) were carried out in a 0.1 M KCl solution with a three-electrode system using the CHI-660 D electrochemical workstation. The platinum foil as the counter electrode, the Ag/AgCl (3 M KCl) as the reference electrode, and the ZnSe-coated ITO substrate were employed as the working electrode. Illumination during EC measurements was provided by a Kessil H150 model 150 W Blue LED light source (390 nm). The electrochemical impedance spectroscopy (EIS) measurements were performed within a frequency range from 100 kHz to 1 Hz at the cathodic potential of 0.05 V with an amplitude of 5 mV.

Results and Discussion

Optical Properties

The UV-Vis spectrometer was used to determine the optical properties of the ZnSe semiconductor thin film. The energy band gap of the ZnSe thin film was determined using the relationship between the absorption coefficient and photon energy as given below:

$$\alpha = A \frac{(h\nu - E_g)^n}{h\nu} \tag{1}$$

Here, α represents the absorption coefficient, A denotes a constant, $h\nu$ stands for the photon energy, E_g represents the energy band gap, and n equals 1/2 because of the direct transition. The plot of α^2 versus $h\nu$ is given in Figure 1. The E_g value of the film was determined by extrapolating the linear portion of the graph onto the energy axis (where $\alpha^2 = 0$). The E_g value of the ZnSe thin film was found as 2.39 eV which below the bulk energy band gap value of ZnSe (2.7 eV) [2-4,11]. There are also studies in the literature where the E_g value is below 2.7 eV [2,4,5,15,17].

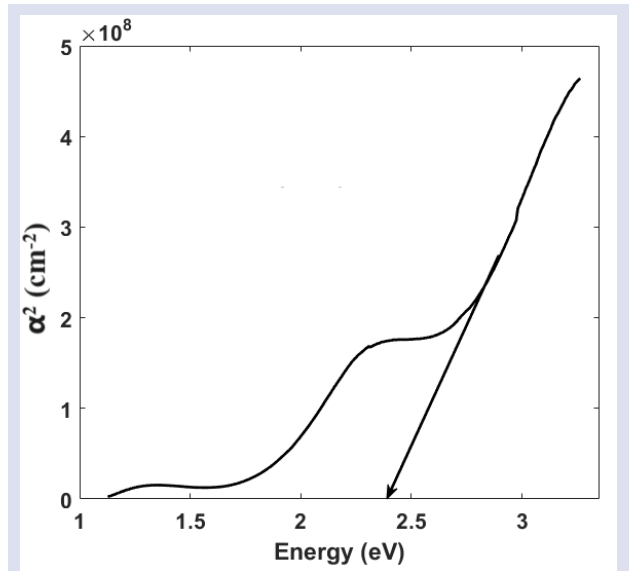


Figure 1. The $\alpha^2 - h\nu$ graphs of the ZnSe thin film on ITO substrate.

Structural Properties

To conduct structural analysis of the ZnSe thin film, XRD measurements were performed scan range from 20° to 80°. The XRD pattern depicting the ZnSe film is presented in Figure 2. The crystal structure and miller indices of the ZnSe film was determined using Joint Committee on Powder Diffraction Standards cards. The diffraction peak at $2\theta \approx 21^\circ$ is related to the ITO (PDF Card No.: 01-089-4598). The diffraction peaks at about 30°, 37°, 50°, and 60° were matched with PDF Card No.: 015-0105 which is expressed to the hexagonal crystal structure of ZnSe. The diffraction peak at about 35° is indicated the hexagonal crystal structure of the ZnSe which matched the 01-073-6558 card number. The peak at $\sim 32^\circ$ was determined to belong to the cubic crystal structure of the ZnSe (PDF Card No.: 01-070-0777). The data obtained indicates that the ZnSe film mostly possesses a hexagonal crystal structure. There are many studies made in aqueous solution by electrodeposition using temperature $\geq 50 \text{ }^\circ\text{C}$. Though most of them has cubic crystal structures [4,5,11,12,15], there are some studies with hexagonal structures [16,17].

The average grain size (D), dislocation density (δ), and strain value (ε) of the ZnSe thin film were calculated by the following equations.

$$D_{hkl} = \frac{K\lambda}{\beta \cos\theta} \tag{2}$$

$$\delta = \frac{1}{D_{hkl}^2} \tag{3}$$

$$\varepsilon = \frac{\beta \cos\theta}{4} \tag{4}$$

K denotes a constant, with a specific value set at 0.9. The parameter β represents the Full Width at Half Maximum (FWHM) measured in radians. The symbol λ signifies the wavelength of the utilized X-ray, while θ denotes the Bragg angle [18–21]. All parameters were calculated for the diffraction peaks observed in the ZnSe thin film and given in Table 1.

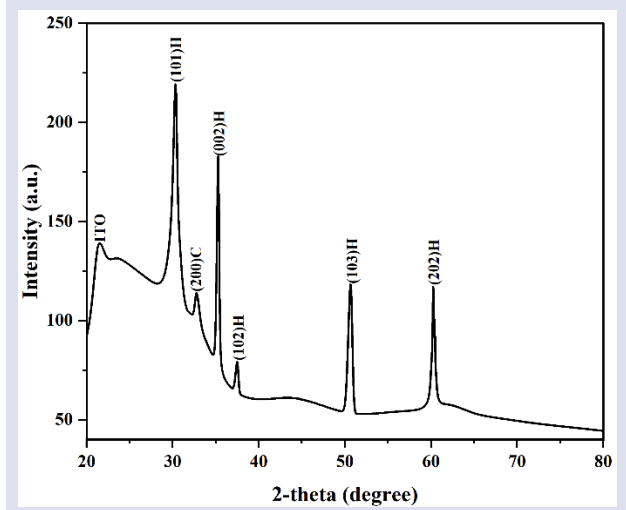


Figure 2. The XRD pattern of the ZnSe thin film on ITO substrate.

Table 1. The average grain size (D), dislocation density (δ), and strain value (ϵ) of the ZnSe thin film on ITO substrate.

(hkl)	Crystal System	D (nm)	δ (10^{15} lines/m ²)	ϵ (10^{-3})
(101)	Hexagonal	11.76	7.228	2.9
(200)	Cubic	7.67	16.99	4.5
(002)	Hexagonal	27.79	1.295	1.25
(102)	Hexagonal	22.68	1.945	1.53
(103)	Hexagonal	16.28	3.775	2.13
(202)	Hexagonal	45.70	0.479	0.76

The vibrational and electronic states of the ZnSe film were investigated by Raman spectroscopy which is providing to characterize the materials with a non-destructive technique. The Raman spectrum of the electrodeposited ZnSe film was given in Figure 3 within the Raman shift range from 150 cm^{-1} to 600 cm^{-1} . There is a peak seen at 249 cm^{-1} attributed to the longitudinal optical (LO) phonon mode of the ZnSe. The LO phonon mode within the range of 238 cm^{-1} – 252 cm^{-1} was reported in earlier studies on electrodeposited ZnSe [3,12,16,17].

Additionally, FT-IR analysis was carried out to further structural analysis. Figure 4 illustrates the FT-IR transmission spectrum of the ZnSe thin film in the wavenumber range of 400 cm^{-1} to 2000 cm^{-1} . The researchers reported that characteristic Zn-Se vibrational modes were observed between 450 cm^{-1} and 1170 cm^{-1} [7–9,22,23]. The peaks observed in the FT-IR spectrum of

the ZnSe thin film at 460, 603, and 744 cm^{-1} correspond to the characteristic Zn-Se vibrational modes.

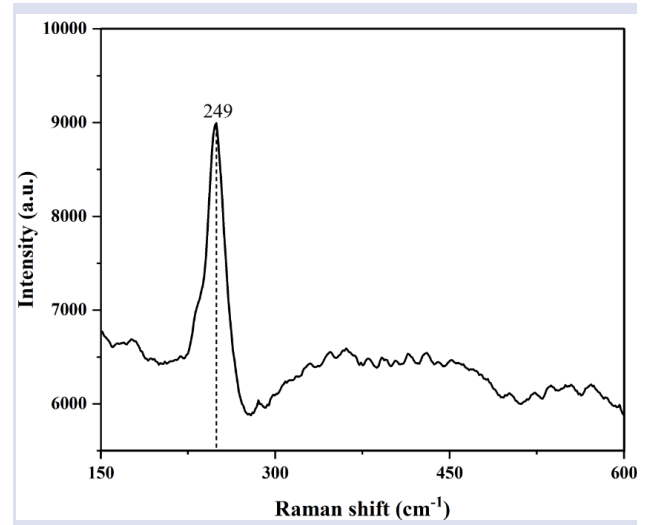


Figure 3. The Raman spectrum of the ZnSe thin film on ITO substrate.

The modes at 460 cm^{-1} and 603 cm^{-1} are attributed to the stretching vibration mode of Zn-Se, and the mode at 744 cm^{-1} represents the bending vibration mode of Zn-Se as given in the earlier studies [2,9,22].

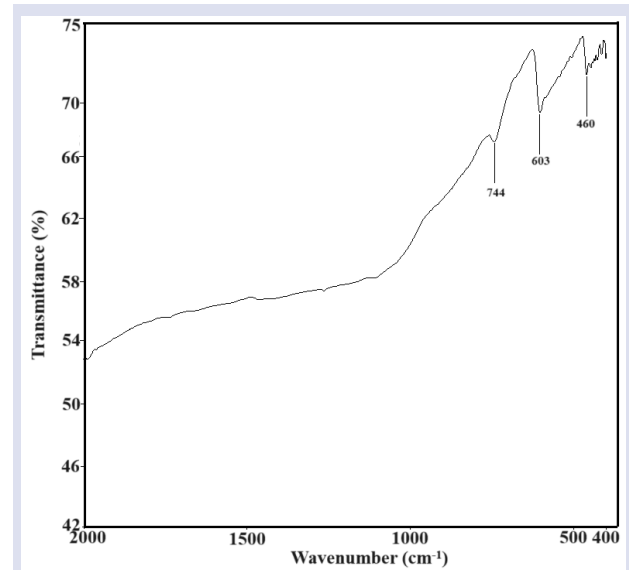


Figure 4. The FT-IR spectrum of the ZnSe thin film on ITO substrate.

Morphological Properties

The morphological properties of the ZnSe film on ITO substrate was investigated by the SEM analysis. Figure 5 presents SEM images of the ZnSe film at magnifications (a) 100.000x and (b) 5.000x. ZnSe film is made up of clusters that contain nanoparticles that range in size from 12 to 32 nm and the image taken at 100.000x magnification in Figure 5 (a) show these clusters. It can be clearly seen from Figure 5 (b) that the ZnSe thin film was deposited on the ITO substrate smoothly and homogeneously.

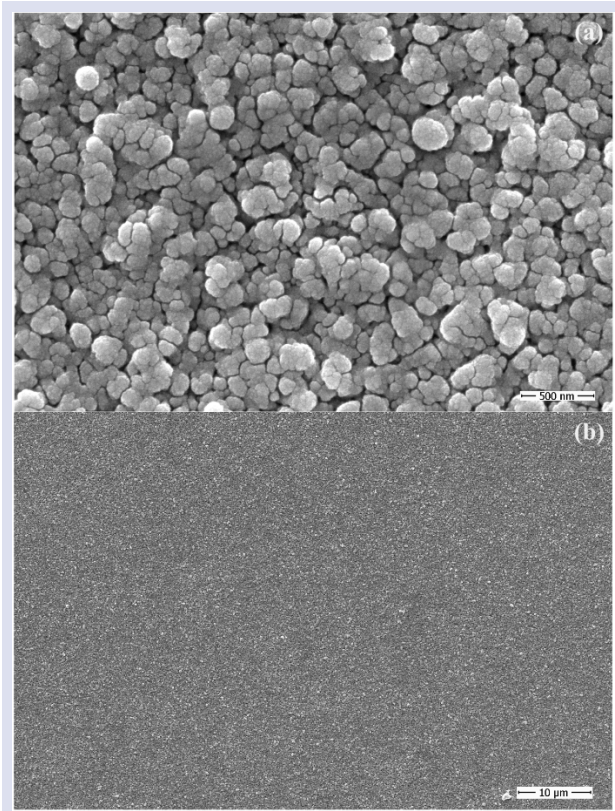


Figure 5. The SEM images of the ZnSe thin film at the (a) 100.000x and (b) 5.000x magnifications.

Electrochemical Measurements

The amperometric measurement was carried out for investigating the photoelectrochemical performance of the ZnSe thin film using the blue LED light (390 nm). Figure 6 shows the photocurrent-time graph obtained from the ZnSe thin film electrodeposited on the ITO substrate in a 0.1 M KCl solution, with the light source being switched on and off. As seen in Figure 6, the ZnSe film exhibited a photoresponse with light illumination and there was a significant increase in photocurrent.

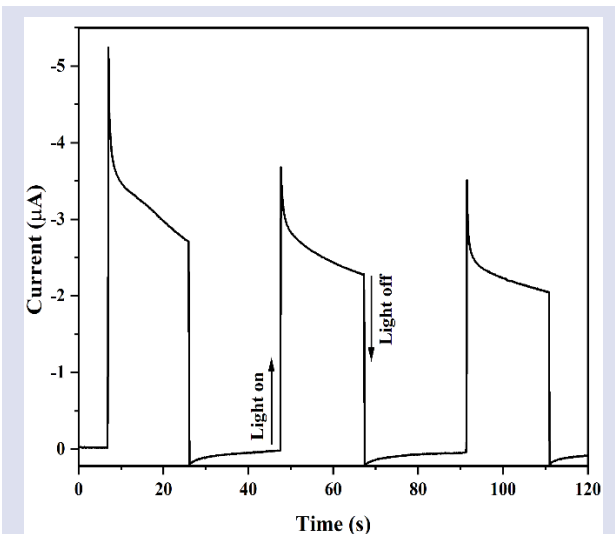


Figure 6. The current-time (I-t) plot of the ZnSe film at light on/off conditions.

Electrochemical impedance spectroscopy (EIS) measurement is a useful technique for investigating charge transfer at the interface between semiconductor and electrolyte. The EIS measurement was performed at open circuit potential (OCP) to determine the charge transport capability under dark and light illumination conditions. The Nyquist plots of the ZnSe thin film both with and without light illumination are shown in Figure 7. The plots of ZnSe have two regions of high-frequency and low-frequency and these plots were fitted with an equivalent circuit as shown in Figure 8. The Zview 2.1b software was used for simulating the Nyquist plots of the ZnSe thin films. The high-frequency region includes an electrolytic resistance (R_e), a charge transfer resistance (R_2) of the ZnSe film, and a doubled layer capacitance (C_1) which occurred interface between the ZnSe thin film/electrolyte. The Warburg (W) impedance which about the diffusion is seen at the low-frequency region. According to the fitting results, R_e decreased from 10.64 Ω to 9.87 Ω, R_2 decreased from 70.76 Ω to 67.27 Ω, and W - R decreased from 989.6 Ω to 586.4 Ω under light illumination.

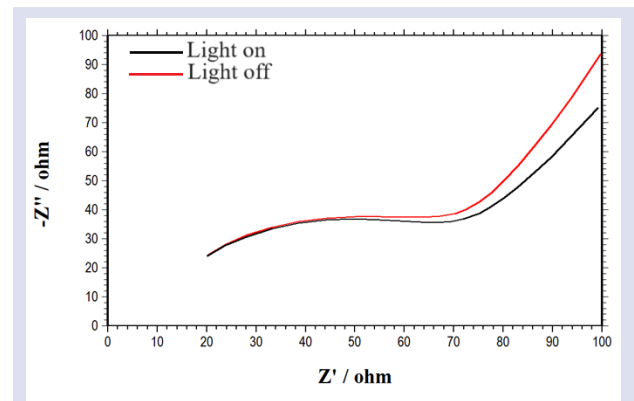


Figure 7. The Nyquist plots of the ZnSe film under light on/off conditions at OCP in 0.1 M KCl.

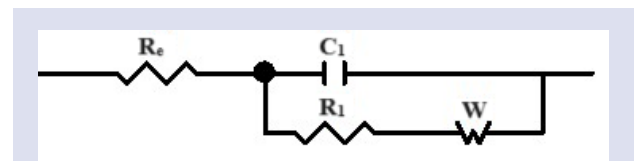


Figure 8. The equivalent circuit for the ZnSe film under light on and off conditions.

To reveal the conductivity type of the ZnSe thin film, Mott-Schottky (MS) analysis was performed with the impedance measurement in the potential range of -0.6 V to 0.1 V. The impedance measurement data was used to plot the potential versus $1/C^2$ graph that is given in Figure 9. The conductivity type of the film was determined based on the shift observed in the MS curve [24–26]. The ZnSe thin film displays a positive shift, indicative of n-type conductivity. Furthermore, the carrier concentration (N_D) and flat band potential (E_F) of the ZnSe was determined from the linear fit of the MS curve using the following equation:

$$\frac{1}{C^2} = \frac{2}{q\epsilon\epsilon_0 N_D} \left[(E - E_F) - \frac{k_B T}{q} \right] \quad (5)$$

C denotes the semiconductor's free charge region, N_D represents the semiconductor's carrier concentration (representing electron donors for n-type or the concentration of hole acceptors for p-type semiconductors), E signifies the applied potential. The determination of N_D was carried out utilizing the slope of the linear fit curve and the E_F was obtained through the extrapolation of the linear fit curve ($1/C^2=0$) [27,28]. The N_D and E_F values of the ZnSe thin film were found as $4.96 \times 10^{11} \text{ cm}^{-3}$ and -1.27 V , respectively.

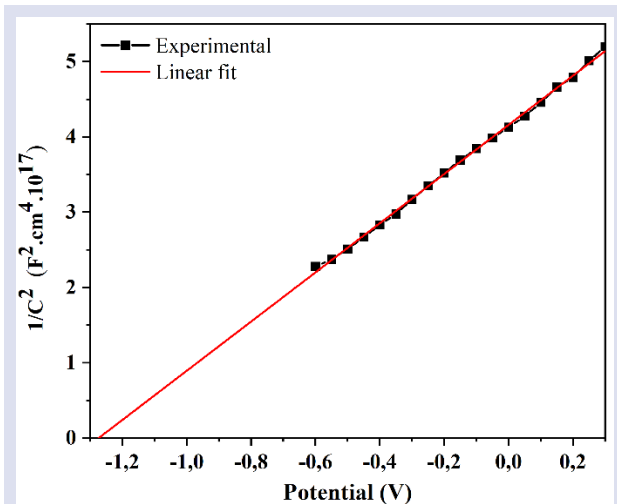


Figure 9. The Mott–Schottky experimental and linear fit curve of the ZnSe thin film.

Conclusion

The ZnSe thin film was synthesized on ITO substrate by electrodeposition technique in an aqueous solution at room temperature. The optical band gap (E_g) of ZnSe was found as 2.39 eV from the UV-Vis measurement, and the crystal structure of the ZnSe thin film matched mostly hexagonal structure by the XRD analysis. It was revealed that by the Raman analysis ZnSe thin film has a peak seen at 249 cm^{-1} associated with the LO phonon mode of the ZnSe, and by the FT-IR transmission spectrum it was seen that the stretching vibration mode and bending vibration mode of Zn-Se. SEM analysis demonstrated that the ZnSe film was made up of clusters that contain nanoparticles that range in size from 12 to 32 nm. The photoelectrochemical performance was investigated with I-t curve and it was obtained that ZnSe film exhibited a photoresponse with light illumination. Also, the value of the R_e , R_2 , and $W-R$ decreased under light illumination. The carrier type, N_D , and E_F values of the ZnSe film were determined as n-type, $4.96 \times 10^{11} \text{ cm}^{-3}$ and -1.27 V , respectively.

Conflicts of interest

There are no conflicts of interest in this work.

References

- [1] Yudin N., Antipov O., Balabanov S., Eranov I., Getmanovskiy Y., Slyunko E., Effects of the Processing Technology of CVD-ZnSe, Cr^{2+} -ZnSe, and Fe^{2+} -ZnSe Polycrystalline Optical Elements on the Damage Threshold Induced by a Repetitively Pulsed Laser at $2.1 \mu\text{m}$, *Ceramics*, 5 (2022) 459–471.
- [2] Lal N., Chawla K., Sharma S., Chouhan R.L., Lal C., Study of electrodeposited zinc selenide (ZnSe) nanostructure thin films for solar cell applications, *Journal of the Indian Chemical Society*, 100 (2023) 101006.
- [3] Prabukanthan P., Kumar T.R., Harichandran G., Influence of various complexing agents on structural, morphological, optical and electrical properties of electrochemically deposited ZnSe thin films, *Journal of Materials Science: Materials in Electronics*, 28 (2017) 14728–14737.
- [4] Gromboni M.F., Mascaro L.H., Optical and structural study of electrodeposited zinc selenide thin films, *Journal of Electroanalytical Chemistry*, 780 (2016) 360–366.
- [5] Dhanasekaran V., Mahalingam T., Rhee J.K., Chu J.P., Structural and optical properties of electrosynthesized ZnSe thin films, *Optik*, 124 (2013) 255–260.
- [6] Yildirim E., Metin Gubur H., Alpdogan S., Ari M., Harputlu E., Ocakoglu K., The effect of annealing of ZnSe nanocrystal thin films in air atmosphere, *Indian Journal of Physics*, 90 (2016) 793–803.
- [7] Khalfi R., Talantikite-Touati D., Tounsi A., Merzouk H., Effect of deposition time on structural and optical properties of ZnSe thin films grown by CBD method, *Opt. Mater.*, 106 (2020) 109989.
- [8] Arslan M., Maqsood A., Mahmood A., Iqbal A., Structural and optical properties of copper enriched ZnSe thin films prepared by closed space sublimation technique, *Mater. Sci. Semicond. Process*, 16 (2013) 1797–1803.
- [9] Ivashchenko M.M., Buryk I.P., Opanasyuk A.S., Nam D., Cheong H., Vaziev J.G., Bibyk V. V., Influence of deposition conditions on morphological, structural, optical and electro-physical properties of ZnSe films obtained by close-spaced vacuum sublimation, *Mater. Sci. Semicond. Process*, 36 (2015) 13–19.
- [10] Boo B.H., Xu N., Lee J.K., Growth of crystalline ZnSe : N thin films by pulsed laser ablation deposition, *Vacuum*, 64 (2002) 145–151.
- [11] Prabukanthan P., Harichandran G., Electrochemical Deposition of n-Type ZnSe Thin Film Buffer Layer for Solar Cells, *J. Electrochem. Soc.*, 161 (2014) 736–741.
- [12] Xu J.L., Gong W.Y., Wang W., Meng H., Zhang X., Shi Z.N., Haarberg G.M., Electrodeposition mechanism of ZnSe thin film in aqueous solution, *Rare Metals*, 36 (2017) 816–820.
- [13] Mahalingam T., Dhanasekaran V., Chandramohan R., Rhee J.K., Microstructural properties of electrochemically synthesized ZnSe thin films, *J. Mater. Sci.*, 47 (2012) 1950–1957.
- [14] Kowalik R., Szaciłowski K., Zabiński P., Photoelectrochemical study of ZnSe electrodeposition on Cu electrode, *Journal of Electroanalytical Chemistry*, 674 (2012) 108–112.
- [15] Asil Uğurlu H., Hamurcu Y., Electrochemical growth of ZnSe thin films, characterization and heterojunction applications, *Mater. Res. Express*, 6 (2019) 116422.
- [16] Lohar G.M., Thombare J. V., Shinde S.K., Han S.H., Fulari V.J., Structural, photoluminescence and photoelectrochemical properties of electrosynthesized

- ZnSe spheres, *Journal of Materials Science: Materials in Electronics*, 25 (2014) 1597–1604.
- [17] Lohar G.M., Shinde S.K., Rath M.C., Fulari V.J., Structural, optical, photoluminescence, electrochemical, and photoelectrochemical properties of Fe doped ZnSe hexagonal nanorods, *Mater. Sci. Semicond. Process*, 26 (2014) 548–554.
- [18] Gubur Metin H., Septekin F., Alpdogan S., CdSe nanowires grown by using chemical bath deposition, *Journal of the Korean Physical Society*, 67 (2015) 1222–1227.
- [19] Ildan Ozmen S., Metin Gubur H., Synthesis and characterization of CdTe/CdSe thin film on glass/ITO by electrodeposition at room temperature, *Bulletin of Materials Science*, 45(2) (2022) 77.
- [20] Ildan Ozmen S., Temiz S.H., Metin Gubur H., Effects of annealing on SnS films produced by chemical bath deposition (CBD), *Phys. Scr.*, 97 (2022) 75704.
- [21] Yildirim E., Ildan Ozmen S., Havare A.K., Gubur H.M., Annealing effect on CdS nanowalls grown by chemical bath deposition on glass substrate, *Phys. Scr.*, 98 (2023) 075933.
- [22] Ivashchenko M.M., Opanasyuk A.S., Buryk I.P., Lutsenko V.A., Shevchenko A.V., Optical properties of pure and Eu Doped ZnSe films deposited by CSVS technique, *Journal of Nano- and Electronic Physics*, 9 (2017).
- [23] Bhagavathula S.D., Kokkarachedu V., Acuna D.Q., Koduri R., Veluri S., Reddy V., Insight of electrical behavior in ferroelectric-semiconductor polymer nanocomposite films of PVDF/ZnSe and PVDF/Cu:ZnSe, *J. Appl. Polym. Sci.*, 134(25) (2017) 44983.
- [24] Baran E., Yazıcı B., Preparation and characterization of poly (3-hexylthiophene) sensitized Ag doped TiO₂ nanotubes and its carrier density under solar light illumination, *Thin Solid Films*, 627 (2017) 82–93.
- [25] Majumder S., Sankapal B.R., Facile fabrication of CdS/CdSe core-shell nanowire heterostructure for solar cell applications, *New Journal of Chemistry*, 41 (2017) 5808–5817.
- [26] Schneider M., Langklotz U., Körsten O., Gierth U., Passive layer investigation on tin and tin solder alloys, *Materials and Corrosion*, (2023) 1-9.
- [27] Baran E., Yazıcı B., Fabrication of TiO₂ -NTs and TiO₂ -NTs covered honeycomb lattice and investigation of carrier densities in I⁻/I³⁻ electrolyte by electrochemical impedance spectroscopy, *Appl. Surf. Sci.*, 357 (2015) 2206–2216.
- [28] Bayramoglu H., Peksoz A., Electronic energy levels and electrochemical properties of co-electrodeposited CdSe thin films, *Mater. Sci. Semicond. Process*, 90 (2019) 13–19.